

## Commissioning of the magnetic diagnostics during the first operation phase at Wendelstein 7-X

K. Rahbarnia<sup>1</sup>, T. Andreeva<sup>1</sup>, A. Cardella<sup>2</sup>, B.B. Carvalho<sup>3</sup>, M. Endler<sup>1</sup>, D. Hathiramani<sup>1</sup>,  
J. Geiger<sup>1</sup>, O. Grulke<sup>1</sup>, S. Lazerson<sup>4</sup>, U. Neuner<sup>1</sup>, J. Svensson<sup>1</sup>, H. Thomsen<sup>1</sup>, A. Werner<sup>1</sup>

and Wendelstein 7-X Team

<sup>1</sup> Max-Planck Institute for Plasma Physics, Wendelsteinstr. 1, 17489 Greifswald, Germany

<sup>2</sup> Fusion for Energy, Boltzmannstr. 2, 85748 Garching, Germany

<sup>3</sup> Instituto de Plasmas e Fusão Nuclear Instituto Superior Técnico, 1049-001 Lisbon, Portugal

<sup>4</sup> Princeton Plasma Physics Laboratory, Princeton, NJ 08540, USA

The set of magnetic equilibrium sensors at the Wendelstein 7-X stellarator (W7-X) in Greifswald, Germany [1, 2] consists of diamagnetic loops, continuous and segmented Rogowski coils and saddle loops (fig. 1 a) [3]. The diamagnetic energy, net toroidal current and moments of the current profiles are targeted. About 50% of the magnetic sensors were operational during the first experimental phase of W7-X (OP1.1) and have been successfully commissioned. Due to the design of the thermal shielding, which has been developed with regard to future long pulse operation (up to 1800s), neither critical heat loads nor thermal damage of the magnetic sensors have been detected. In the present contribution first measurement results will be discussed.

An automatized, multi-channel data recording system, as well as corresponding data evaluation software tools have been developed and established. The individually adapted sensor design and a corresponding electrical shielding scheme ensure low signal noise levels and high signal integration accuracy.

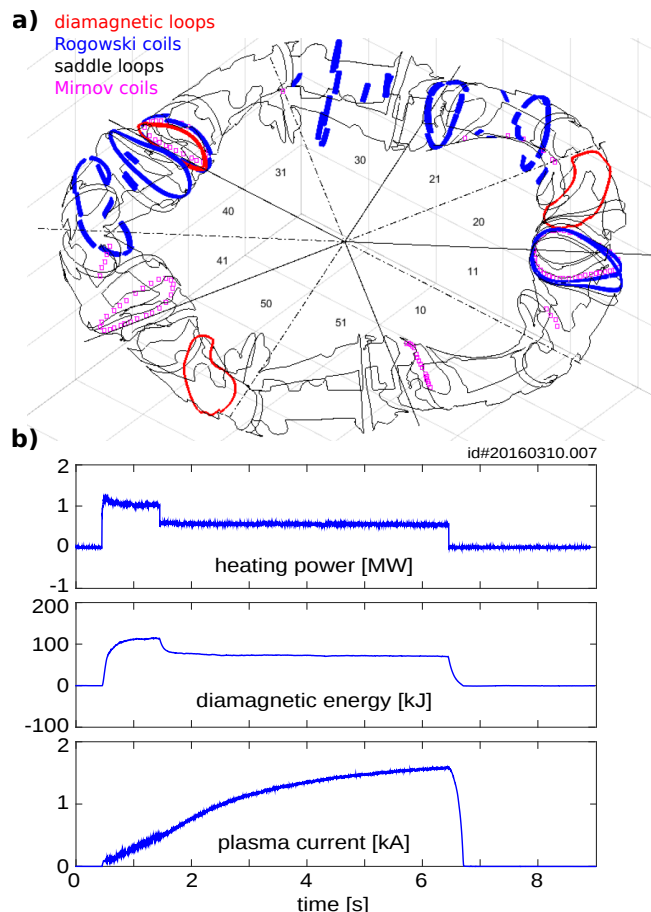


Figure 1: a) Magnetic diagnostics at Wendelstein 7-X b) Measurements of the diamagnetic energy and plasma current during a 6 s hydrogen plasma with  $T_e \approx 5$  keV and  $n_e \approx 2 \times 10^{19} \text{ m}^{-3}$ .

In fig. 1 b time traces of evaluated data recorded during a 6 s hydrogen plasma are depicted.

The compensated diamagnetic energy measured by the diamagnetic loop (triangular shaped plasma cross-section) remains constant after plasma build up. The total toroidal plasma current measured by the continuous Rogowski coil (triangular shaped plasma cross-section) rises until the plasma heating stops and the plasma collapses. First estimates of confinement times in typical hydrogen plasmas are of the order of 100–200 ms. These values are similar compared to data analysis results involving electron temperature and density profile data from the Thomson scattering diagnostic. They are also comparable to predictions based on empirical scaling laws, like ISS04 [4].

Current fluctuations in the main superconducting field coil system and currents, which are induced in the plasma vessel, affect the measurement of the diamagnetic energy. A compensation of the main diamagnetic loop in the triangular shaped plasma cross-section is performed via a set of four compensation coils located in the vicinity of the main loop (insert in fig. 2 a). The compensation coils do not encircle the plasma and can therefore be used to correct the signal of the main diamagnetic loop for non-plasma related magnetic flux changes. A calibration for the compensation has been performed during a predefined current ramp of 15 A/s in the main field coils without plasma recording the magnetic fluxes of the diamagnetic loop ( $\phi_{dia}$ ) and the compensation coils ( $\phi_{comp}^i$ ). During the ramp a calibration factor  $C$  is determined under the assumption of  $\phi_{dia} - C \sum \phi_{comp}^i \stackrel{!}{=} 0$ . The compensated diamagnetic energy can then be derived approximately as  $W_{dia} = -\mu_0 \Phi / (3\pi R_0 B_0)$  [5] with the major radius  $R_0$ , the magnetic field  $B_0$  and the com-

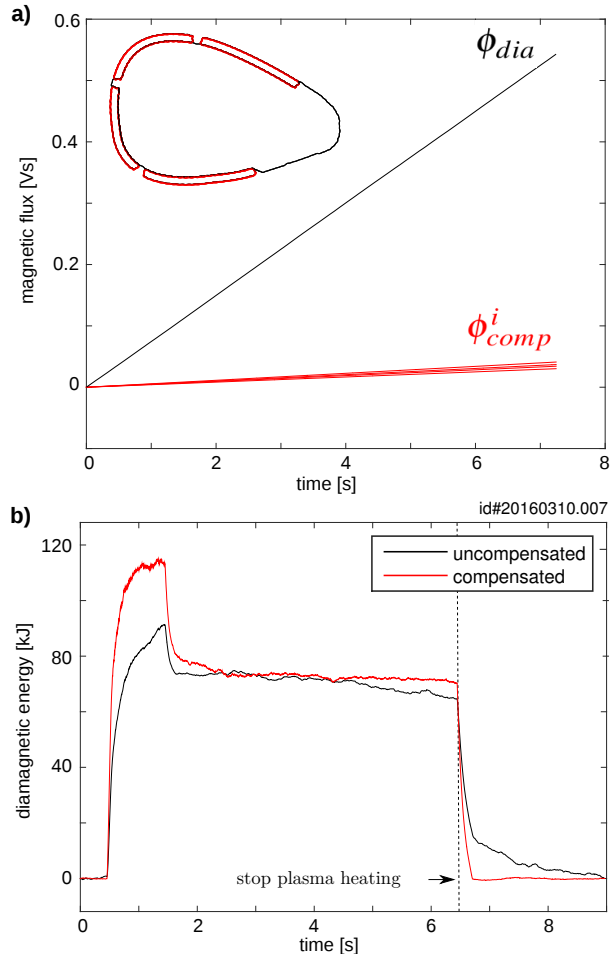


Figure 2: a) Measured magnetic fluxes during a current ramp in the superconducting magnet system. The arrangement of diamagnetic main loop (black) and compensation coils (red) is shown in the embedded sketch. b) Direct comparison of uncompensated and compensated measured diamagnetic energy as described in the text.

netic loop for non-plasma related magnetic flux changes. A calibration for the compensation has been performed during a predefined current ramp of 15 A/s in the main field coils without plasma recording the magnetic fluxes of the diamagnetic loop ( $\phi_{dia}$ ) and the compensation coils ( $\phi_{comp}^i$ ). During the ramp a calibration factor  $C$  is determined under the assumption of  $\phi_{dia} - C \sum \phi_{comp}^i \stackrel{!}{=} 0$ . The compensated diamagnetic energy can then be derived approximately as  $W_{dia} = -\mu_0 \Phi / (3\pi R_0 B_0)$  [5] with the major radius  $R_0$ , the magnetic field  $B_0$  and the com-

pensated diamagnetic flux  $\Phi = \phi_{dia} - C \sum \phi_{comp}^i$ . In fig. 2 a the measured magnetic fluxes of the diamagnetic loop and the compensation coils during the calibration are depicted.

The determined calibration factor  $C \approx 7.65$  agrees within 1% with corresponding Biot-Savart calculations. The effect of the net toroidal plasma current on the presented diamagnetic energy estimation is found to be less than 1%.

The derived compensated diamagnetic energy is shown in Fig. 2 b in comparison with the corresponding uncompensated signal. During the plasma build-up phase an expected faster response time in the compensated signal is observed. Residual effects due to influences mentioned above can clearly be seen in the uncompensated signal after the plasma heating stops. An improved compensation scheme taking into account a small plasma effect on the compensation coils is currently under development.

A number of Rogowski coil segments have been installed at W7-X mainly to obtain information on plasma current distributions. An arrangement of eight segments in the triangular shaped plasma cross-section is depicted in fig. 3 a. Due to the gaps between the segments the sum of the measured signals is expected to be slightly smaller when compared to the continuous Rogowski coil signal in the triangular shaped plasma cross-section, which has been experimentally confirmed (fig. 3 b). However the individual segment signals show a clear dipolar structure, as depicted in fig. 3 c, which mainly corresponds to the related Pfirsch-Schlüter-current pattern in the plasma.

A rough calibration of the diamagnetic loops, saddle loops and Rogowski coils has been done.

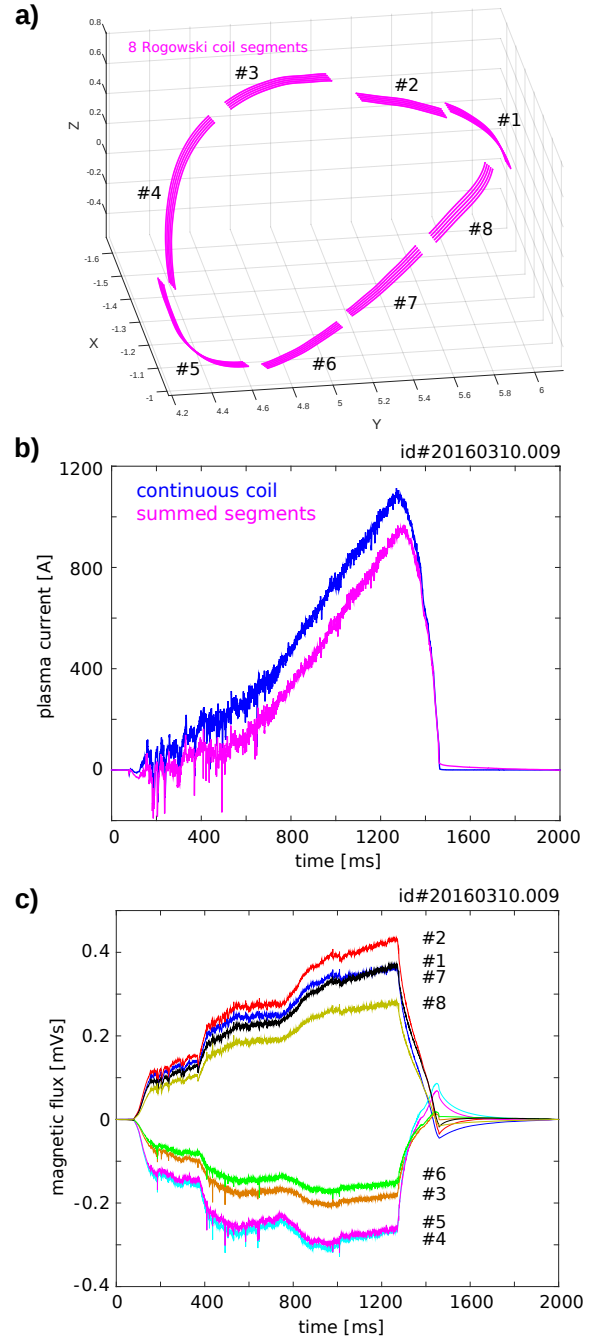


Figure 3: a) Arrangement of eight Rogowski segments; b) The sum of the signals is slightly smaller compared to the signal of the continuous Rogowski coil. c) Individual magnetic fluxes of Rogowski segments

For that purpose the corresponding magnetic flux changes were recorded during previously defined current ramps in the trim coils of W7-X. A calibration matrix was derived by comparing the sensor responses to mutual inductances calculated with the DIAGNO code [6, 7]. First equilibrium reconstructions based on the calibrated magnetic measurements have been successfully performed by using VMEC [8] and STELLOPT [9, 10]. A combined reconstruction based on magnetic measurements as well as plasma profile data of electron cyclotron emission and Thomson scattering diagnostics is currently being implemented. A precise calibration of the continuous Rogowski coils is planned for the time prior to the next campaign using a current conductor being temporally installed in the vacuum vessel.

For investigating magnetohydrodynamic modes, Alfvén modes and edge localized modes a set of 125 Mirnov coils has been installed (fig. 1 a). During OP1.1 four of them located in the triangular shaped plasma cross-section next to the diamagnetic loop could be put into operation. Fig. 4 shows data of a single Mirnov coil spectrogram measured during the previously shown 6 s hydrogen plasma. A clear mode activity at about 7 kHz is found, which has been also observed with various other diagnostic systems, like electron cyclotron emission measurements and correlation reflectometry. Possible mode locations and associated mode numbers are currently being investigated.

This work has been carried out within the framework of the EUROfusion Consortium and has received funding from the Euratom research and training programme 2014-2018 under grant agreement No 633053. The views and opinions expressed herein do not necessarily reflect those of the European Commission.

## References

- [1] C. Beidler et al., *Fusion Technol.*, **17**, 148 (1990)
- [2] H.-S. Bosch et al., *Nucl. Fusion* **53**, 126001 (2013)
- [3] M. Endler et al., *Fusion Eng. and Design*, **100**, 468 (2015)
- [4] H. Yamada et al., *Nucl. Fusion*, **45**, 1684 (2005)
- [5] S. Besshou et al., *Nucl. Fusion*, **26**, 1339 (1986)
- [6] S. Lazerson et al., *Plasma Phys. Control. Fusion* **55**, 025014 (2013)
- [7] H.J. Gardner, *Nucl. Fusion* **30**, 1417 (1990)
- [8] S.P. Hirshman et al., *Comput. Phys. Commun.* **43**, 143 (1986)
- [9] S. Lazerson et al., *Nucl. Fusion*, **55**, 023009 (2015)
- [10] D.A. Spong et al., *Nucl. Fusion* **41**, 711 (2001)

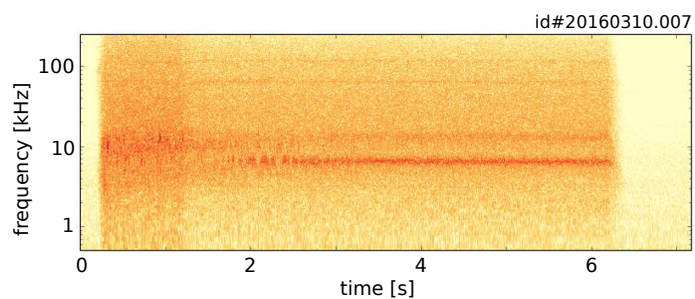


Figure 4: The spectrogram measured by a selected Mirnov coil clearly shows activity around 7 kHz, but also at higher frequencies around 100 kHz.